

Statistical modelling of structural and thermodynamical properties of vitreous B₂O₃

This article has been downloaded from IOPscience. Please scroll down to see the full text article.

1995 J. Phys.: Condens. Matter 7 8035

(<http://iopscience.iop.org/0953-8984/7/42/002>)

View [the table of contents for this issue](#), or go to the [journal homepage](#) for more

Download details:

IP Address: 171.66.16.151

The article was downloaded on 12/05/2010 at 22:17

Please note that [terms and conditions apply](#).

Statistical modelling of structural and thermodynamical properties of vitreous B_2O_3

M Micoulaut†, R Kerner† and D M dos Santos-Loff‡

† Laboratoire GCR-CNRS URA 769, Université Pierre et Marie Curie, T 22-12, Boite 142, 4 Place Jussieu, 75252 Paris Cédex 05, France

‡ Departamento de Matemática, Universidade de Coimbra Apartado 3008, 3000 Coimbra, Portugal

Received 30 March 1995, in final form 23 August 1995

Abstract. We present in this paper a thermostatical model of formation of vitreous B_2O_3 which is based on a description of agglomeration of BO_3 triangles resulting in medium-range clusters and on the construction of the partition function related to the space of all possible pathways leading to this set of clusters. With one fitted parameter which is the boroxol formation energy of 5.3 ± 0.7 kcal mol⁻¹, the model predicts the usual shape of the internal energy function and the heat capacity curves, as well as the fraction of boroxol rings of 83%. In the last section, we investigate the structural evolution of molten B_2O_3 during the glass transition process.

1. Introduction

The boron oxide is one of the oldest known glass-forming materials. The very easy production of this compound and the fact that this glass is one of those supporting the basic 'continuous random network' model of Zachariasen [1], have led to numerous studies, both theoretical and experimental, in various fields of investigation [2].

The stoichiometry of vitreous boron oxide (a III–VI compound) suggested long ago that its structure could be represented as a three-dimensional continuous random network (CRN) with BO_3 triangles, which was confirmed by means of x-ray and neutron diffraction [3, 4]. Indeed, the diffraction patterns show two very sharp peaks at 1.37 and 2.37 Å, corresponding to the B–O and O–O distances in the equilateral BO_3 triangle, whereas other much broader peaks clearly suggest that there are no edge-sharing units in the glass (like a four-membered ring, B_2O_4), whereas considerable evidence was obtained for the existence of larger structural groups, namely six-membered rings B_3O_6 , called boroxol rings, composed of three corner-connected BO_3 triangles (figure 1). This assumption was later confirmed by the analysis of Raman spectra which exhibit a high vibrational peak at 808 cm⁻¹ (attributed to the breathing mode of the oxygens inside the boroxol rings [5, 6]) and whose intensity and sharpness is comparable to those of usual crystals, suggesting that the network is mainly composed of randomly oriented boroxol rings connected by oxygen atoms or BO_3 triangles.

Several other experiences realized during the past fifteen years also seem to confirm the hypothesis. Jellison and co-workers who applied ¹⁷O NMR spectroscopy to *v*- B_2O_3 , constructed a model of oxygen sites inside and outside boroxol rings, which explained that the best agreement with experiment can be obtained assuming that as many as 83% of the borons are trapped inside the boroxol rings [7].

^{18}O enriched compounds have also been analyzed in order to show that the breathing mode of the oxygens inside the boroxol rings at 808 cm^{-1} is strongly modified by the isotopic substitution and follows the isotope rate [8]. Similar work has been done on vitreous and molten B_2O_3 by Walrafen *et al* investigating especially the temperature dependence of the integrated Raman intensity of the 808 cm^{-1} peak [9]. They have observed that the sharp peak disappears with increasing temperature, suggesting a general breakdown of the boroxol groups in the liquid. These authors have also shown that the formation of a boroxol ring might be energetically favoured and have measured a corresponding formation energy of 5 kcal mol^{-1} [10].

Last but not least, neutron and inelastic neutron diffraction results can be entirely interpreted by assuming a high fraction of boroxol rings; Johnson *et al* have concluded the rate to be 60% [11], Hannon *et al* give the evaluation of $80 \pm 5\%$ [12, 13].

Controversy around boroxol rings started with the publication of numerous molecular dynamics (MD) simulations in recent years [14, 15, 16]. Various modelling methods of MD have been used, such as two-body potentials, and three-particle interactions with the bond angle maintained at 120° or 130° . All of them, except one, predict the absence of boroxol units in the network, or rate at least a very small number.

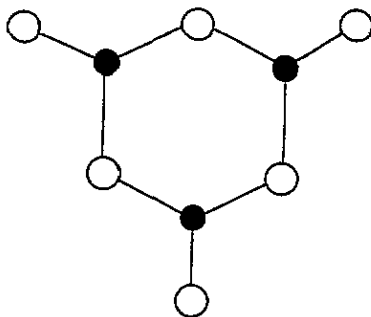


Figure 1. The boroxol group.

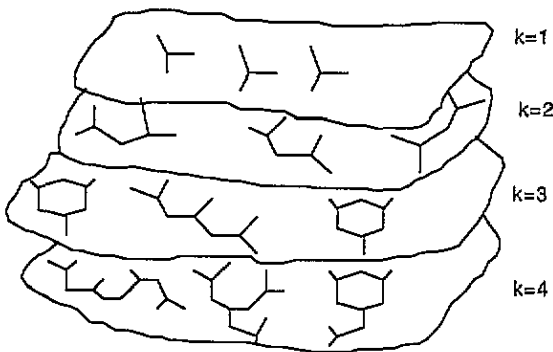


Figure 2. The different sheets of configuration space containing all clusters of given size N .

In this article, we shall apply a simple statistical model of agglomeration to the vitreous boron oxide, in order to evaluate the number of boroxol rings. In the next two sections, the main theoretical ingredients of the model are presented. These are the set of rules of cluster agglomeration, the way to compute corresponding probabilities and the construction of the partition function. The results are shown and discussed in the fourth section. The number of constructed clusters increases so rapidly during the successive steps of agglomeration that we shall introduce what we call the *multiplet approximation* which will be explained in the fifth section. Due to this approximation, more precise results can be obtained, in particular for the boroxol rate. The last section is devoted to the structural analysis of molten B_2O_3 . We evaluate the temperature dependence of the maximal size of clusters coexisting at a given temperature in the glass-forming liquid. This investigation relies strongly on Walrafen's data [9].

2. Description of the theoretical model

Before we proceed with detailed calculations, let us expose the main lines along which our model is constructed, describing the purely qualitative picture that serves as the theoretical support. Although theories of irreversible thermodynamical processes are known, [17], they are too general to be of much use here. That is why we shall employ a simple model of agglomeration and growth introduced in our previous articles [18, 19, 20].

The main idea of the model is based on the following simple observation. In the hot liquid many types of microcluster coexist in a dynamical equilibrium as long as the temperature is constant; some of them split into smaller entities, some agglomerate and grow a little bit, but on average the overall statistics remains constant, i.e. the probability of finding a cluster of given type does not vary, although the particular distribution of the probabilities depends very strongly on local geometry and the energy cost of their formation. This equilibrium is broken as soon as the temperature starts to vary: as it decreases, the smaller clusters agglomerate producing bigger ones; the overall picture is that of a time-dependent distribution of different clusters, its centre of gravity drifting towards the bigger ones. At some moment—corresponding to what is observed as the glass transition—the clusters attain their ‘critical size’, after which the statistical distribution of any characteristic quantity (in our case it will be the fraction of boron atoms trapped inside the boroxol rings) becomes stationary, i.e. attains its limiting value observed in the network as a whole.

Our approach to the mathematical description of this process is based on the image displayed in figure 2. We divide the configuration space of all possible clusters observed in the hot melt into a series of sheets, numbered from 1 to N_{max} , each of them containing only the clusters of a given size k ($k = 1, 2, \dots, k_{max}$).

The aim of this article is to establish the way in which the elementary growth and agglomeration processes occur when the temperature slowly goes down during the glass transition. To do so, we follow the growth patterns of all possible agglomeration processes, starting with the simplest one, which is the creation of a single oxygen bridge between two boron atoms; during the next step of agglomeration two possibilities must be accounted for, namely, creation of a chain of three borons, or a ring containing three boron atoms; these two ‘pathways’ have different statistical weights due to the different number of ways (*multiplicities*) with which these arrangements can occur; besides, the relative weights should contain the Boltzmann factors corresponding to the different energy costs involved. After normalizing by the sum of the obtained weights we get the probabilities of each of these configurations; then, we can start again and obtain all the four-boron clusters, and so on. From the distribution of probabilities evaluated in this way, we can compute other characteristic features, e.g. the rate of the boron atoms becoming trapped inside the boroxol rings. Because the probabilities depend on the temperature via Boltzmann factors, we can also obtain the temperature behaviour of this characteristic. The overall normalization factors for the probability distribution of clusters can be used as the partition function, although they refer rather to the *processes* and not the states. We show that this approximation gives a reasonable description of the resulting structures and of the glass transition process as well.

Let us explain our approach in a more detailed manner.

A hot melt at constant temperature contains a lot of clusters of different sizes and shapes, although one can assume that there is a more or less sharp cut-off in size at some $k_{max}(T)$, i.e. that the number of clusters bigger than $k_{max}(T)$ is negligibly small in a hot liquid. Of course, in a quasiequilibrium, at a given constant temperature, some of the clusters split into smaller units, while some of the smaller ones agglomerate giving bigger entities, but

on average the balance is maintained, and the mean distribution of clusters on the sheets of the configuration space remains unchanged.

But let the temperature go down slowly, and the distribution of probabilities of finding a given number of clusters of given type on a k th sheet will also evolve; the lower the temperature, the greater the 'population' of clusters corresponding to greater values of k . It is quite obvious that when the temperature continues to go down, the centre of gravity of the overall distribution will also displace itself towards the sheets of greater k ; at the same time, the cut-off size value k_{max} is growing, too.

This situation is similar to that of a mixture of different kinds of molecule with chemical reactions between them allowed to happen: there we do not know the chemical potentials of each species, which could have been used to produce the statistical sum. That is why we choose the alternative description based on the pathways, which produce the probabilities for each species without explicit introduction of a particular chemical potential. In the limit of growing k_{max} , the renormalizing factors of this procedure should be close to the big statistical sum.

In order to apply this kind of non-standard statistical physics, we should be convinced that the system under study satisfies the following physical hypotheses.

(1) The progression of the population of clusters from one sheet to another due to the agglomeration and growth is slow as compared with the kinetic energy exchange between the clusters (i.e. with the speed of phonons in the hot liquid). Therefore, although the whole process is off equilibrium, we may assume a thermodynamical equilibrium on each of the sheets, and use the Boltzmann factors there.

(2) The clusters in the hot melt are in constant proximity, and their movements are not as rapid as the motion of the molecules in a gas; consequently, we shall assume that the probability of collisions is roughly constant, i.e. depends very weakly on the temperature, so that the most important contribution to the probability of a given agglomeration step is given by the statistical weight (i.e. the number of ways in which this step can be performed) and the Boltzmann factor depending on the energy cost of that particular process.

(3) We shall consider the energies stored in a given cluster during its agglomeration as additive quantities, which is equivalent to supposing that the energy is locally conserved. This means that we can evaluate the probability of observing a given cluster by summing up all the agglomeration pathways that lead to its creation from elementary singlets, by multiplying the probabilities of each transition by corresponding statistical weights and Boltzmann factors.

The non-standard character of our procedure can be illustrated as in figure 3.

With this in mind, we can proceed further and start to evaluate the probabilities of all possible agglomeration pathways and their overall normalizing factors, which will be interpreted as successive approximations to quasipartition functions.

3. Construction of multiplets and quasipartition function

The model is based on the geometrical construction of all possible small- and medium-size clusters containing a given number of atoms (up to 15 borons and 20 oxygens), starting from the most elementary configuration for which there exists clear and unambiguous experimental evidence, i.e. the BO_3 triangle, which will be called a singlet in the forthcoming construction [21]. During the agglomeration of the singlets, the boron atom and its three oxygen bonds form oxygen bridges with next borons.

Although we can safely assume that the network can be entirely tiled with these singlets,

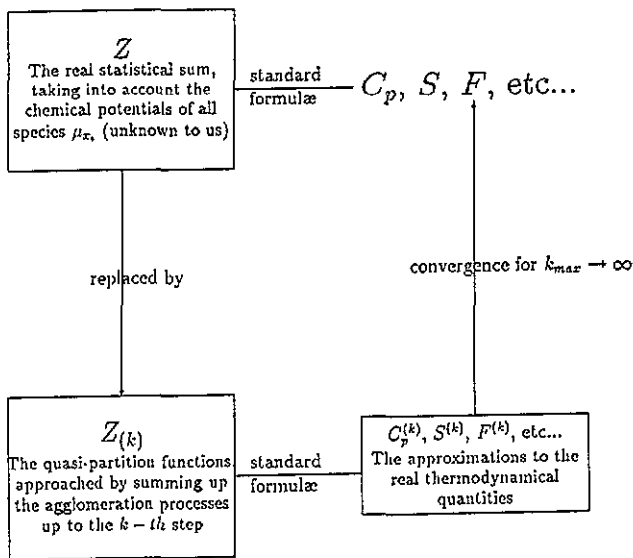


Figure 3. The alternative way of evaluating C_p , S , F , etc.

the vitreous matrix of B_2O_3 which has undergone a glass transition can be tiled also with larger agglomerates produced by our construction, each step of agglomeration yielding larger clusters and a better approximation, because the final medium-range structures we shall produce obviously contain more significant information about the typical structure of B_2O_3 than the initial doublets and triplets. Whatever the construction step, contribution to the configurational entropy coming from a given cluster can be evaluated with a satisfactory approximation by computing the number of independent agglomeration pathways leading to that particular cluster. Besides the entropy contribution, we can assume that the energy stored in a given cluster can be treated as an additive quantity and can be evaluated by summation of the energies involved in each elementary step of agglomeration consisting in the formation of a new single oxygen bridge or of two simultaneous bridges (corresponding to the creation of a boroxol ring).

We cannot exclude in this construction either the formation of a random network with BO_3 triangles or a boroxol linked network, because the processes that lead to such structures are characterized by two unknown binding energies we shall evaluate later on. Each single oxygen bridge creation should represent the energy cost of E_1 and each boroxol creation the energy E_2 . Starting from a BO_3 singlet, we can create a doublet out of two singlets (figure 4) and exclude the possibility of formation of a two-membered ring (i.e. edge-sharing triangles), for which there is no experimental evidence in x-ray results, because they would produce in the diffraction pattern a sharp and characteristic peak which is not observed [3]. Therefore, the probability of the doublet after normalization is $p_{2A} = 1$ and we can tile the whole network with such doublets.

During the second step ($l = 2$), two possibilities must be taken into account, i.e. formation of a pure chain or of a boroxol ring (figure 5). Besides the energies E_1 and E_2 that characterize these two processes, the two triplets have a different multiplicity (degeneracy), which corresponds to the number of ways in which a given triplet can be constructed. A boroxol group has the multiplicity $2 \times 3 \times 4 = 24$, whereas for a chain we count $3 \times 4 = 12$. Indeed, for the latter, there are 12 different ways to join a singlet with

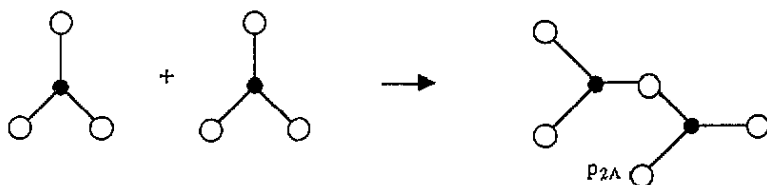


Figure 4. From a singlet to a doublet p_{2A} .

a doublet via a single oxygen bridge, if one labels the bridges (e.g. $l-l'$, $l-k'$, $l-m'$, etc) (figure 5).

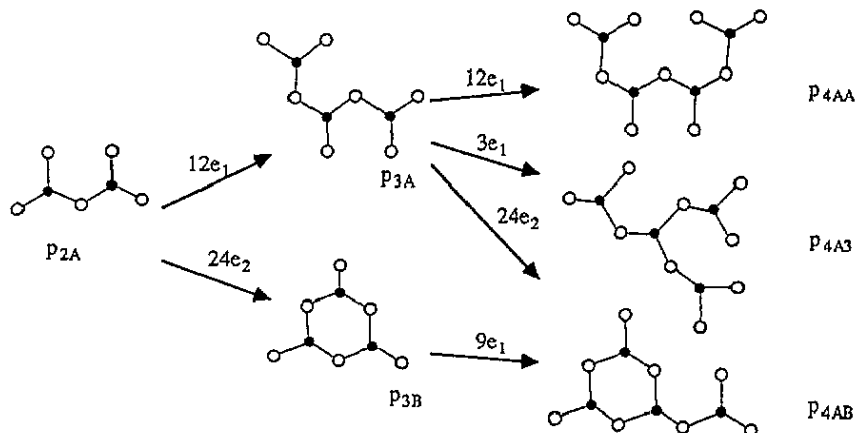


Figure 5. The construction of triplets and quadruplets, starting from the doublet p_{2A} .

The simplest way to evaluate the probabilities of these two structural states with the corresponding binding energies E_1 and E_2 is the description by means of canonical ensemble summations:

$$p_{3A} = \frac{12e_1}{12e_1 + 24e_2} p_{2A} = \frac{1}{1 + 2e_2/e_1} \quad (1)$$

$$p_{3B} = \frac{24e_2}{12e_1 + 24e_2} p_{2A} = \frac{2e_2/e_1}{1 + 2e_2/e_1} \quad (2)$$

where $e_1 = \exp[-E_1/kT]$ and $e_2 = \exp[-E_2/kT]$.

The next step leads to three different multiplets: their multiplicities and the Boltzmann factors e_1 and e_2 of each pathway of production are shown in figure 5 and the normalized probabilities are given below:

$$p_{4AA} = \frac{12e_1}{15e_1 + 24e_2} p_{3A} = \frac{4}{5 + 8e_2/e_1} p_{3A} \quad (3)$$

$$p_{4A3} = \frac{3e_1}{15e_1 + 24e_2} p_{3A} = \frac{1}{5 + 8e_2/e_1} p_{3A} \quad (4)$$

$$p_{4AB} = \frac{24e_2}{15e_1 + 24e_2} p_{3A} + \frac{9e_1}{9e_1} p_{3B} = \frac{8e_2/e_1}{5 + 8e_2/e_1} p_{3A} + p_{3B}. \quad (5)$$

We can go on with this construction and for each new step produce a set of multiplets with the corresponding probabilities. Each new step l costs at least one new binding energy, so

that the stored energies contained in a given multiplet are given by the following accessible states:

$$E_j^{(l)} = (l - j) E_1 + j E_2 \quad j \in \left\{ 0, \left[\frac{l+1}{3} \right] \right\}. \quad (6)$$

Note that this construction depends only on the energy difference $E_1 - E_2$ (via the factor e_2/e_1), and that the quadruplets displayed in figure 5 involve only two characteristic energies, $E_1^{(3)} = 3E_1$ and $E_{11}^{(3)} = 2E_1 + E_2$. We have followed the agglomeration up to the 10th step yielding 288 non-redundant multiplets with 11 boron atoms each (table 1).

Table 1. The number of multiplets at each step of the agglomeration process.

Step l	Number of multiplets	Number of multiplets with:		
		1 boroxol	2 boroxols	3 boroxols
0	1	—	—	—
1	1	—	—	—
2	2	1	—	—
3	3	1	—	—
4	4	2	—	—
5	9	4	1	—
6	14	6	2	—
7	31	14	6	—
8	62	30	13	1
9	135	60	34	4
10	288	129	74	15

Some of them contain one, two or three boroxol rings; some others contain no rings at all and are composed of pure or ramified chains. Rings with more than four boron atoms should also be expected in our construction but we have neglected them for the sake of simplicity. Nevertheless, such rings can be represented by a pure chain, because it seems reasonable to assume that the energetic cost of formation of such rings is approximately twice the energy E_1 (during the l th step, a pure chain with $(l - 2)$ borons is 'closed' by a BO_3 triangle). Such an assumption becomes more and more realistic if one considers rings of growing size (the effect of the ring decreases with its size, i.e. the influence of a three-membered ring is more significant than the one produced by a 12-membered ring). Therefore, the main structural influence should be produced by the boroxol rings represented by E_2 state energies; two examples of clusters with 11 boron atoms are given in figure 6. The first one is a typical example of an artificial ring (or pure chain), whereas the second one contains three boroxol groups.

As the probabilities of each multiplet are constructed in the same way as the probabilities of 'classical ensemble state' energies with Boltzmann factors and their corresponding degeneracy, the overall normalizing factors which appear in equations (1)–(5), but also in the forthcoming steps of agglomeration, should imitate the behaviour of a statistical sum, i.e. a partition function which uses different combinations of the energies E_1 and E_2 stored in a given cluster (6), as classical ensemble state energies.

Nevertheless, such a computation would be very approximate because the degeneracy of a given energy state would be much higher than the ordinary statistical weight of agglomeration. In other words, if one takes care only of the states defined in (6), one does not make any difference among multiplets with the same stored energy (e.g. the quadruplets

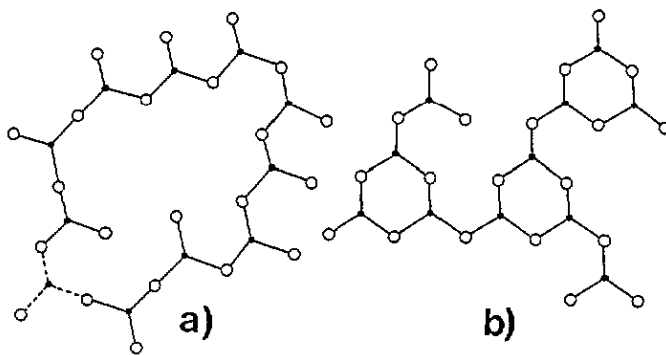


Figure 6. (a) A pure chain which could eventually close in order to produce a ring, state energy $E_{10}^{(10)} = 10E_1$. (b) A cluster containing three boroxol rings, state energy $E_3^{(10)} = 7E_1 + 3E_2$.

of figure 5 p_{4A} and p_{4A1} have the same energy state, which is $3E_1$). That is why the 'partition function' $Z_{(m)}$ should not refer to an ensemble of momentaneous states of the same system, but rather to an ensemble of 'evolution processes' (or pathways) that lead to the set of all clusters of given size m . In this sense, the obtained statistical sum does not refer to a system in an equilibrium thermodynamical state, but rather enables us to use a similar technique for a non-equilibrium irreversible process such as the glass transition we want to describe.

We are conscious of the non-standard character of this procedure and of the fact that the formal expressions for the thermodynamical quantities such as C_p and S do not correspond to the real values of these functions measured experimentally during the glass transition or derived from the classical partition function, were we able to compute it. Nevertheless, we believe that the estimations obtained in this manner tend to the realistic ones with growing length of pathways taken into consideration, which corresponds to the extension of the fictitious phase space of the melt to include more and more sheets displayed in figure 2. One of the reasons to believe that it is so comes from the inspection of the relative weight of the contribution of the N th sheet, which can be evaluated roughly from the number of species of clusters of size N (see table 1), where we see that due to the geometric character of the progression in number of configurations, the relative weight of the last sheet is roughly equivalent to the weight of all the previous sheets ($N - 1$, $N - 2$, etc).

We believe that the progression of clusters from sheet to sheet corresponds to what happens in the hot melt during glass transition, as described in section 2.

Another reason which seems to us to corroborate the validity of the approach is that our obtained thermodynamical functions computed from our quasipartition function $Z_{(m)}$ exhibit a characteristic feature, i.e. the slope of C_p at the glass transition temperature is increasing with growing size of clusters (figure 8) and for an infinite size, we expect an infinite slope in agreement with the usual behaviour of C_p .

Although correlations in the configuration of neighbouring cluster pairs should be sensitive to their shapes and space-filling properties, we believe that, at the level of approximation we are using here, the steric hindrances are not very important in determining the glass transition temperature and the behaviour of C_p . The geometrical properties of the clusters become crucial while discussing the behaviour of density or viscosity during glass transition; the behaviour of C_p , on which our model is most dependent, is much less influenced by the steric exclusions that can be observed in the formation of bigger clusters. Therefore, although one may be concerned that the 'book-keeping' of pathways

is not so evidently correct, because the agglomeration rates, besides statistical weights and Boltzmann factors, could depend on correlations in the configurations of neighbouring cluster pairs, we believe that these correlations introduce only minor modifications into the thermodynamic location of the glass transition. It can be argued *a posteriori* that the steric hindrances coming from the big closed chains (like figure 6(a)) are negligible because the rate of formation of these chains is very low as compared with the boroxol rings, which geometrically behave all in a quite similar manner.

Now we are ready to evaluate the successive approximations to the quasipartition function. For example, for the second step (which yields the triplets p_{3A} and p_{3B}), the partition function has the simple form (see equations (1) and (2)):

$$Z_{(2)} \sim 12 e^{-E_1/kT} + 24 e^{-E_2/kT}. \quad (7)$$

For the third step, the construction is quite similar:

$$Z_{(3)} \sim \prod_{\alpha=1}^2 Q_{\alpha}^{(3)} = 9e_1(15e_1 + 24e_2). \quad (8)$$

For further steps, the partition function can be written in the same way:

$$Z_{(l)} \sim \left[2\pi M_{(l+1)} k_B T \right]^{3N_{(l+1)}/2} \prod_{\alpha=1}^{N_{(l)}} Q_{\alpha}^{(l)} \quad (9)$$

where $N_{(l)}$ is the initial number of multiplets (clusters) of the step l and $N_{(l+1)}$ the number of created multiplets during this step, $M_{(l+1)}$ the atomic mass of a structure with $l+1$ boron atoms and $Q_{\alpha}^{(l)}$ the normalizing factor of the pathway labelled α ($\alpha = 0, \dots, N_{(l)}$); k_B stands for the Boltzmann constant. The first factor results from the usual integration of the kinetic energy term of the partition function (contribution of classical harmonic oscillators). One can now evaluate the normalized internal energy of a given step l :

$$U_{(l)} = \frac{3}{2} k_B T + \frac{1}{N_{(l+1)}} k_B T^2 \frac{\partial}{\partial T} \sum_{\alpha=1}^{N_{(l)}} \ln Q_{\alpha}^{(l)} \quad (10)$$

and the heat capacity C_p by the derivation with respect to T :

$$C_p^{(l)} = \frac{3}{2} k_B + \frac{1}{N_{(l+1)}} \left(2k_B T \frac{\partial}{\partial T} + k_B T^2 \frac{\partial^2}{\partial T^2} \right) \sum_{\alpha=1}^{N_{(l)}} \ln Q_{\alpha}^{(l)}. \quad (11)$$

4. Results

We shall study the system of clusters constructed above and its thermodynamical functions $U_{(l)}$ and $C_p^{(l)}$ in the vicinity of the glass transition, although it seems probable that the heat capacity should take into account other contributions (e.g. the rotational or vibrational modes' contribution to the kinetic energy terms in the partition function); but we shall assume that the most important contribution to the behaviour of $C_p^{(l)}(T)$ is fairly well approximated by the second and third terms of equation (11).

Although the characteristic quantities of a liquid such as α_T , C_p or κ_T (bulk compressibility) might be discontinuous at T_g suggesting a manifestation of a second-order or a more complex phase transition, we can nevertheless expect the presence of an inflexion point in the curve of the heat capacity at this temperature, which should reflect what is generally observed in the $C_p(T)$ curve for various glass-forming systems [22]:

$$\frac{\partial^2}{\partial T^2} \left[C_p^{(l)} \right]_{T=T_g} = 0. \quad (12)$$

This simple requirement will be used in order to fit the parameter ($E_1 - E_2$) of our model and to satisfy equation (12). Nevertheless, the glass transition temperature is a function of the thermal history of the melt which is highly influenced by the cooling (or quenching) rate. The usual glass transition's temperature range for B_2O_3 is known to be approximately 470–530 K. Trying to fit the energy difference $E_1 - E_2$ in order to satisfy equation (12), we obtain different values following the choice varying from $T_g = 470$ K to 530 K, which suggests that our value $E_1 - E_2$ might need a correction whose value would depend on the cooling rate, but which can be neglected as long as the cooling rate is slow enough in order to influence in the same way all particular agglomeration processes taken into account.

For $T_g = 470$ K, we obtain the best fit for steps (3)–(10) for

$$E_1 - E_2 = 0.200 \text{ eV} = 4.605 \text{ kcal mol}^{-1} \quad (13)$$

and for $T_g = 530$ K

$$E_1 - E_2 = 0.260 \text{ eV} = 5.986 \text{ kcal mol}^{-1}. \quad (14)$$

The corresponding normalized internal energy and heat capacity curves based on these numeric values of $E_1 - E_2$ are plotted in figures 7 and 8 for the consecutive steps of agglomeration.

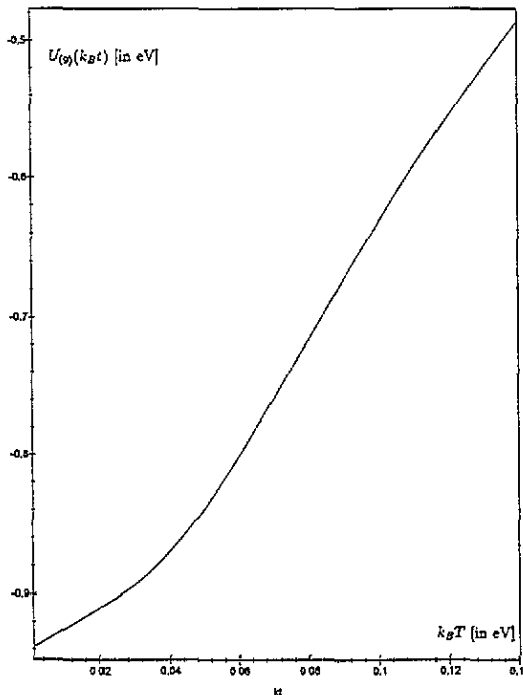


Figure 7. Normalized internal energy curve $U_{(g)}(T)$ (in eV) with $E_1 - E_2 = 0.26$ eV.

The energetic difference $E_1 - E_2$ obtained here is in fair qualitative agreement with previously cited theoretical and experimental estimates.

4.1. Comparison with other estimates

Snyder has estimated by means of *ab initio* quantum mechanical calculations the energy difference between BO_3 groups in boroxol rings compared with the energy of BO_3 groups

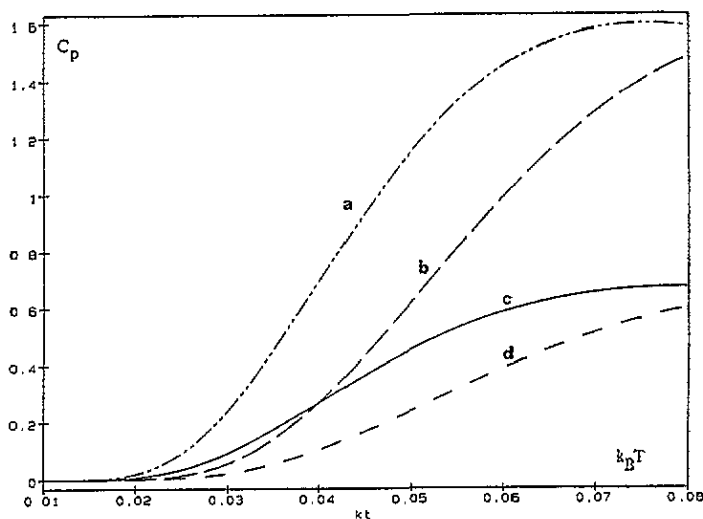


Figure 8. Normalized heat capacity curve (reduced units) for different steps of agglomeration ($l = 8$ (curves *a* and *b*) and $l = 9$ (curves *c* and *d*)) with $E_1 - E_2 = 0.20$ eV and $E_1 - E_2 = 0.26$ eV. The plot concerns only the second term of equation (11), which is the most significant.

in a random network. Although the first rough approximation gave a relatively low value of about $\Delta E = 1.5$ kcal mol⁻¹, the corrections taking into account the electron correlation energy raised this value up to 6 kcal mol⁻¹ [23].

Krogh-Moe has proposed the stabilization energy of a boroxol unit to be roughly 8 kcal mol⁻¹ after discussing the reorganization of BO_3 units from boroxol rings into a random network of BO_3 triangles [24].

Walrafen and co-workers have proposed the value 6.4 ± 0.4 kcal mol⁻¹, which has been deduced from the investigation of vitreous and molten B_2O_3 via computation of the dependence of the integrated Raman intensities on the temperature [9].

The mean value obtained by our statistical model (5.3 kcal mol⁻¹) is in very good agreement with the most recent result which has been obtained by the extended work of the latter cited authors. Indeed, they have estimated the energy of formation of a boroxol unit as being roughly equal to 5.0 kcal mol⁻¹ [10].

4.2. The boroxol rate

With the energy difference established and the glass transition temperature fixed, we can compute the fraction $F_{(l)}$ of boron atoms trapped inside the boroxol rings by summing the probabilities of clusters containing this characteristic structural group, with an appropriate weight, e.g. $\frac{3}{4}$ for the configuration p_{4AB} of figure 5 or $\frac{9}{11}$ for the structure displayed in figure 6(b), etc. The results exhibit behaviour converging to the limit value of 80%; the continuous curve extrapolating the behaviour of $F_{(l)}$ versus l (from 1 to 10) is plotted in region I of figure 9. The obtained rate is consistent with various theoretical and experimental results which have been presented in the first sections of this paper, especially with the models of Jellison *et al* who suggested that 83% of boron atoms are contained in boroxol rings [7] and Hannon *et al* (80%) [12, 13].

The evaluation of the boroxol rate and its dependence on T also shows that for $T = T_g$ the variation of $F_{(l)}$ is very low; note that this happens whatever the agglomeration step we

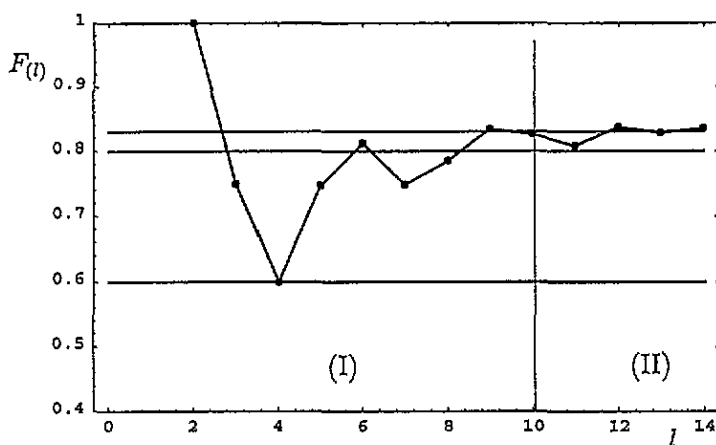


Figure 9. The obtained boroxol rate: region I, direct joining of singlets; region II, multiplet approximation. The horizontal lines represent the values established by Jellison *et al* [7], Johnson *et al* [11] and Hannon *et al* [12, 13].

are considering. When the liquid gets frozen at T_g , all structural recombination of clusters is stopped (or at least becomes negligibly slow); this is confirmed by our computation, in which our functions $F(l)$ remain constant from $T = -200$ °C up to T_g which is consistent with the experimental data of Walrafen [9, 10].

Nevertheless, at this stage of agglomeration, the amplitude of the variations in the boroxol rate computed for different steps, even for the last ones (steps 9–10 in figure 9) remain quite important. Therefore, it seems necessary to go farther in the agglomeration process, in order to evaluate the boroxol rate from larger clusters in a more precise and conclusive manner.

5. Construction of larger clusters: the multiplet approximation

We have already seen that the agglomeration steps could provide various reasonable pieces of information from the analysis of structures containing up to 11 boron atoms. For the ultimate step of agglomeration ($l = 10$) that we were able to follow exactly, we have 288 non-redundant multiplets, and it seems quite impossible to perform the analysis of the agglomeration process further by direct joining of BO_3 triangles ‘by hand’. Indeed, the forthcoming step $l = 11$ would provide at least a thousand non-redundant multiplets with 12 boron atoms which would prove very difficult to follow without important redundancy errors. Luckily enough, at this stage of the agglomeration ($l = 10$), we can compute all the probabilities of all 288 multiplets by inserting the T_g value and its corresponding best fit for the difference $E_1 - E_2$. (By the way, we have checked that there is no significant variation of probability between the two values of T_g .) It is noteworthy that among the 288 multiplets, only very few are really significant, i.e. have a non-negligible probability. For example, the multiplets displayed in figure 6 have very different probabilities. The pure chain shown in (a) has the probability of 10^{-19} whereas the second structure in (b), appears with a 37.8% rate!

We shall denote by ‘multiplet approximation’ the method which keeps only the most representative multiplets of a step l and starts a new agglomeration by direct joining of BO_3 singlets to these multiplets only. Of course, the sum of the probabilities of the thus-reduced

number of multiplets should always be greater than 99% in order to minimize the error produced by the approximation. Anyhow, structures with a very low probability (such as the one shown in figure 6(a)) will produce pathways with infinitesimal probabilistic weight, unimportant for the construction of larger clusters during forthcoming steps, whereas the structures whose development we decided to follow will continue to lead to the really meaningful ones.

In order to test the validity of such an approximation, we have started the multiplet approximation at step $l = 9$ which has a population of 135 multiplets (table 1). With the value $E_1 - E_2$ obtained in (13) and (14), only five of these multiplets represent 99.11% of all the probabilities (table 2). We can now realize a new step of agglomeration (called 10*), computing the probability of the 12 structures with 11 borons, obtained from the five most important multiplets of the previous step, and compare them with the probabilities of the direct computation based on the 288 multiplets of step 10.

Table 2. The number of different structures obtained by the multiplet approximation compared to the directly computed ones.

Step l	Number of multiplets	Number of multiplets with	
		2 boroxols	3 boroxols
9	135	34	4
	5	3	2
10*	12	7	5
10	288	74	15

The very low difference in the probabilities of multiplets obtained via the approximate and exact way of agglomeration (10 and 10*) confirms that such an approximation is valid, as long as one retains the multiplets that would total about 99% of all the probabilities (table 3). Having tested the validity of this approximation, we can now confidently apply it further and continue the agglomeration process by constructing the multiplets with 12 boron atoms, starting from the six most representative multiplets at step 10. A second multiplet approximation can be realized in order to obtain structures with 15 boron atoms during the steps labelled 13** and 14** (table 4) if we start from the 11 most representative clusters with 13 boron atoms (which represent 99.10% of all the probabilities).

With these new agglomeration steps, we are able to compute again the fraction of borons inside boroxol rings, following the same scheme as explained above. The result is plotted in region II of figure 9 and shows a much better convergence for steps 11* to 14** to approximately 84% which remains in good agreement with the value established by Jellison *et al* [7] and stays inside the evaluation range of Hannon and co-workers [12, 13]. The variation of $F_{(l)}$ with respect to l is also decreasing, as shown in figure 9.

6. The microanalysis of glass transition

Let us return to the analysis of the agglomeration process, trying now to evaluate its time dependence, i.e. the way in which the characteristic features, that can be evaluated statistically on the microclusters considered above, approach their limit values evaluated in the resulting network after the glass transition has been completed. This will enable us to analyse the evolution of the agglomeration process as a function of time and temperature, assuming that the latter may be considered as a linear function of time.

Table 3. The multiplet approximation test: the probabilities of the 12 most significant clusters obtained with the approximation during step 10* compared to the most representative multiplets obtained by direct joining (step 10).

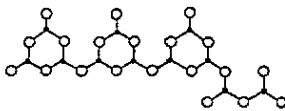
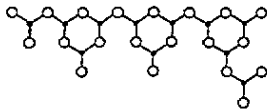
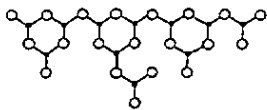
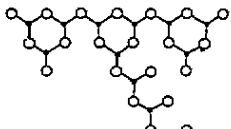
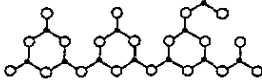
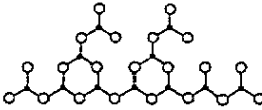
Direct computation $l = 10$	Multiplet approximation $l = 10^*$	
0.1748	0.1740	
0.1743	0.1740	
0.3782	0.3780	
0.0859	0.0852	
0.1472	0.1472	
0.0306	0.0306	

Table 4. The number of structures sharing from 11 to 15 boron atoms, by use of the two multiplet approximations.

Step l	Number of multiplets	Number of multiplets with			
		2 boroxols	3 boroxols	4 boroxols	5 boroxols
10	288	74	15	—	—
	6	1	5	—	—
11*	17	4	11	2	—
12*	39	8	26	5	—
	11	—	8	3	—
13**	32	—	23	10	—
14**	93	—	62	29	2

We have at our disposal the statistics of microclusters of all possible types containing up to 11 boron atoms, and a good approximation up to 15 boron atoms per cluster. The main question to be answered now is: what is the relative weight of the full ensemble of clusters containing the given number of boron atoms among all the clusters present in the melt,

and how does this distribution of probabilities evolve with time (or, what is roughly the same, with temperature)? In other words, we would like to know how the whole population of multiplets travels from one sheet of the configurational space to another, as described qualitatively in the second section of this article. We shall show how the quasigeometric progression of the number of different types of multiplet with growing l finds its image in the exponential behaviour of the average cluster size as a function of temperature, and in the exponential approach of the boroxol ring statistics towards its limit value. Incidentally, it will give us an idea of the *critical size* of clusters, at which all the significant statistics are almost identical with the overall statistics that characterize the 'frozen' network resulting from the glass transition that has definitively taken place.

Although in the pure B_2O_3 glass we have only one characteristic parameter at our disposal, i.e. the rate of boron atoms contained in the boroxol rings, it can be used in order to decipher the unknown statistics of clusters of given type.

Walrafen *et al* give the experimental curve describing the temperature dependence of the integrated intensity of the sharp 808 cm^{-1} peak (attributed to the boroxol breathing mode) which is proportional to the boroxol rate $F(T)$ [9] and has been modelled by these authors with the following function:

$$\ln \left(\frac{F(T)}{B_0 - F(T)} \right) = \frac{3237.66}{T} - 2.58893 \quad (15)$$

where B_0 is the boroxol rate at T_g . With the characteristic energy differences established above, our model enables us to compute the boroxol rate $F_{(k)}$ averaged over all clusters of a given size k ; this quantity is also a function of temperature T which enters via the set of Boltzmann factors contained in the expression of $F_{(k)}$.

Now, in order to produce a more realistic picture, we must take into account that the melt contains a mixture of clusters of all sizes up to some N_{max} that grows with time as the temperature goes down. The problem is how to evaluate the relative part of the clusters of size k , for $k = 1, 2, \dots, N_{max}$. What is helpful here is the following simple observation: if the agglomeration pace is roughly the same at any point of the melt, it means that it takes the same characteristic time for a cluster of size k to transform into a cluster of size $k + 1$. This means in turn that the ratio of the number of clusters of size $k + 1$ to the number of clusters of size k is roughly given by the ratio of the numbers of possible multiplets given in table 1. The numbers N_k of different multiplets containing k boron atoms grow as 1-1-2-3-4-9-14-31-62-135-288-..., which is very close to the geometric progression with the constant ratio close to 2.13; if we weight the numbers of multiplets with the numbers of boron atoms contained in them, i.e. if we consider the series kN_k , the progression is even more impressive.

One should not forget the crucial dependence on the energies displayed in the Boltzmann factors, because the result is very sensitive to their variation. This could easily be checked by examining the changes in figure 10 when one varies the energies E_i , even slightly. The resulting curves (figure 10) depend also on the characteristic energies.

This means that, to a first approximation at least, the most important contribution to any statistics will come from the last and biggest type of cluster. That is the reason why we propose to evaluate theoretically the boroxol rate with a simple formula

$$F_{N_{max}}(T) = \frac{1}{N_{max}} \sum_{k=1}^{N_{max}} F_{(k)}(T) \quad (16)$$

which will give a good approximation if N_{max} could be evaluated as a function of temperature.

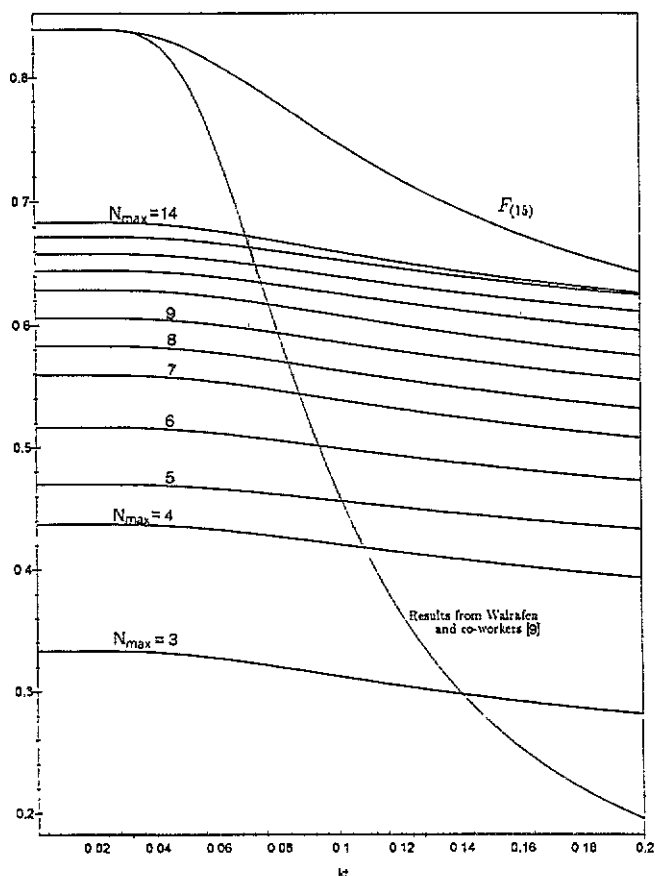


Figure 10. The experimental curve of Walrafen *et al* [9] and the curves $F_{N_{max}}(k_B T)$ with $E_1 - E_2 = 0.20$ eV. $F(k_B T)$ has been plotted with the limit value $B_0 = 0.84$ in order to be consistent with $F_{(15)}$ and figure 9.

But this is exactly what we can get if we plot on the same graph all the curves $F_{N_{max}}(k_B T)$ and the experimental curve $F(k_B T)$ of Walrafen *et al* with the limit value $B_0 = 0.84$ (figure 10). The intersection points between the theoretical curves corresponding to different values of N_{max} and the experimental curve tell us at what temperature the approximation with a given N_{max} is the best; this in turn can be read as the dependence of N_{max} on T (figure 11(a)).

The points displayed in figure 11(a) are very well iterated by an exponential with a constant:

$$k_B T = A + B e^{-\lambda N_{max}} \quad (17)$$

with $A = 0.0628$ eV, $B = 0.0966$ eV, $\lambda = 0.1897$ for the choice 13. We see that when the maximal size of clusters considered attains 15 borons, the corresponding temperature is close to 0.07 eV, i.e. still above the real glass transition temperature.

In parallel, we can draw the development of the boroxol rate with temperature by projecting the same intersection points on the vertical axis of figure 10; this gives another exponential approach to the limiting value of 84% (figure 11(b)). We believe that this exponential behaviour is also reflected in the exponential (i.e. very rapid) behaviour of other

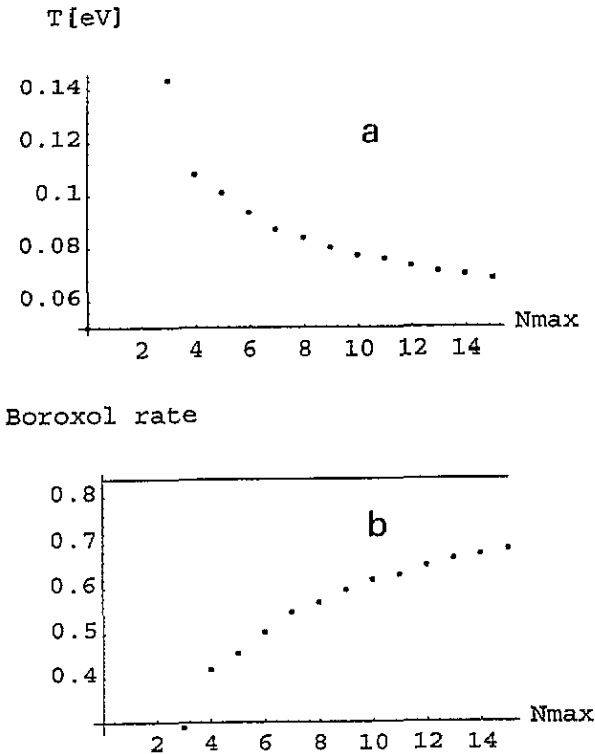


Figure 11. (a) The dependence of T (in eV) on N_{max} , the maximal size of a cluster in the considered set, with $E_1 - E_2 = 0.20$ eV. (b) The boroxol rate as a function of N_{max} . The horizontal line represents the limit value of 0.84%.

interesting parameters, above all, of the viscosity, which should have a typical Arrhenius behaviour like similar strong glass-forming systems [25].

7. Conclusions

The fact that with a simple thermostistical model, based on the topological construction of large clusters, we can obtain the usual shape for $C_p(T)$ and $U(T)$ curves, the realistic values for the energy of creation of a boroxol ring (5 kcal mol^{-1}) and a very satisfying fraction of boroxol rings (84%). Besides these typical results for vitreous and molten B_2O_3 , this paper is a first attempt at a model in order to give a microscopic description of the glass transition. These are the positive features of the model that will encourage us to perform a similar analysis on other glass-forming systems, including SiO_2 [26].

Acknowledgments

The authors are grateful to Nick Rivier (University of Strasbourg, France) and Adrian C Wright (University of Reading, UK) for useful advice; they are also greatly indebted to Rafael A Barrio (UNAM, Mexico) and Jim C Phillips (AT&T Bell Laboratories, USA) for very interesting discussions and comments. D M dos Santos-Loff was supported by a grant from the JNICT, Portugal.

References

- [1] Zachariassen W H 1932 *J. Chem. Phys.* **54** 3841
- [2] Phillips J C 1979 *J. Non-Cryst. Solids* **34** 153
- [3] Mozzi R L and Warren B E 1970 *J. Appl. Crystallogr.* **3** 251
- [4] Goubeau J and Keller H 1953 *Z. Anorg. (Allg.) Chem.* **272** 303
- [5] Galeener F L, Lucovski G and Mikkelsen J C Jr 1980 *Phys. Rev. B* **22** 3983
- [6] Barrio R A, Castillo-Alvarado F L and Galeener F L 1991 *Phys. Rev. B* **44** 7313
- [7] Jellison G E Jr, Panek L W, Bray P J and Rouse G B Jr 1977 *J. Chem. Phys.* **66** 802
- [8] Windish C F and Risen W M 1982 *J. Non-Cryst. Solids* **48** 307
- [9] Walrafen G E, Samanta S R and Krishnan P N 1980 *J. Chem. Phys.* **72** 113
- [10] Walrafen G E, Hokmabadi M S, Krishnan P N and Guha S 1983 *J. Chem. Phys.* **79** 3609
- [11] Johnson A V, Wright A C and Sinclair R N 1982 *J. Non-Cryst. Solids* **50** 281
- [12] Hannon A C, Sinclair R N and Wright A C 1993 *Physica A* **201** 375
- [13] Hannon A C, Grimley D I, Hulme R A, Wright A C and Sinclair R N 1994 *Proc. Pacific Rim Meeting (Hawaii); J. Non-Cryst. Solids* **175**
- [14] Soules T F and Varshneya A K 1981 *J. Am. Ceram. Soc.* **64** 145
- [15] Soppe W and den Hartog H W 1989 *J. Phys. C: Solid State Phys.* **21** L689
- [16] Teter M P 1987 *Am. Ceram. Soc. Bull.* **66** 562
- [17] Keizer J 1987 *Statistical Thermodynamics of Nonequilibrium Processes* (Berlin: Springer)
- [18] Kerner R and dos Santos D M 1988 *Phys. Rev. B* **37** 3881
- [19] Kerner R and Micoulaut M 1994 *J. Non-Cryst. Solids* **176** 271
- [20] Kerner R 1991 *J. Non-Cryst. Solids* **135** 155
- [21] dos Santos-Loff D M, Micoulaut M and Kerner R 1994 *Europhys. Lett.* **28** 573
- [22] Elliott S R 1990 *Physics of Amorphous Materials* (New York: Longman)
- [23] Snyder L C 1978 *Quantum Mechanical Studies of the Structure and Thermochemistry of Species Postulated to Exist in Borate Glasses; Am. Ceram. Soc. Mtg. (Bedford Springs, 1978)*
- [24] Krogh-Moe J 1969 *J. Non-Cryst. Solids* **1** 269
- [25] Angell C A 1988 *J. Non-Cryst. Solids* **102** 205
- [26] Kerner R 1995 *J. Non-Cryst. Solids* **182** 9